Author/s:
Vincent, CL;Huang, Y

Title:
Meso- and microscale response to variation in cloudiness at three forested sites in the Maritime Continent

Date:
2022-01-01

Citation:
Vincent, C. L. & Huang, Y. (2022). Meso- and microscale response to variation in cloudiness at three forested sites in the Maritime Continent. Quarterly Journal of the Royal Meteorological Society, 148 (742), pp.418-433. https://doi.org/10.1002/qj.4212.

ORIGINAL ARTICLE

Meso- and micro-scale response to variation in cloudiness at three forested sites in the Maritime Continent

Claire L. Vincent[1,2] | **Yi Huang**[1,2]

[1]School of Geography, Earth and Atmospheric Sciences, The University of Melbourne

[2]ARC Centre of Excellence for Climate Extremes

Correspondence
Claire Vincent, School of Geography, Earth and Atmospheric Sciences, The University of Melbourne, Parkville, 3010, Victoria, Australia
Email: claire.vincent@unimelb.edu.aum

Funding information
ARC Centre of Excellence for Climate Extremes (CE170100023) ; ARC Discovery Project Scheme (DP190100786)

This study examines the relationships between the diurnal precipitation cycle, local morning insolation and local and large-scale moisture availability using local radiative flux and precipitation observations from three forested tropical sites, together with ERA5 reanalysis data. Our results suggest that away from the coast, there is a weak positive correlation between local morning insolation and the magnitude of the afternoon precipitation peak, and a weak negative relationship between locally observed surface moisture in the morning and the magnitude of the afternoon precipitation peak. There is little relationship between large-scale column moisture and the local afternoon precipitation peak.

We examine analogous results in convection permitting simulations. Results suggest that the simulated afternoon precipitation-rate shows almost no dependence on surface radiative forcing or moisture availability, while observed afternoon precipitation-rate is dominated by radiative forcing. Simulated and observed satellite precipitation and cloud estimates for a single case study suggest a diversity of surface-flux-precipitation relationships amongst model configurations.

Abbreviations: SOM, Self Organising Map; PSO, Pasoh Forest Reserve; BKS, Bukit Soeharto; PDF, Palangkaraya Drained Forest site.

* Equally contributing authors.

KEYWORDS
Diurnal precipitation cycle, Tropical Convection, Surface fluxes, Mesocale modelling

1 | INTRODUCTION

The onset and intensity of tropical convection is a balance of moisture availability, and thermodynamic and kinematic forcing. While moisture availability is an obvious pre-requisite to convection, it has been shown that in tropical coastal regions, precipitation can occur at relatively lower mid-tropospheric moisture levels than over the open ocean [1]. This effect is hypothesised to be due to enhanced kinematic and thermodynamic forcing related to the seabreeze circulation.

While the total column moisture has been shown to be closely related to precipitation [2] on monthly and daily scales, the surface conditions play an important role in locally determining moist parcel ascent. For example, Thomas et al. [3] showed that the surface moisture was inverse-linearly related to the lifting condensation level at a tropical site on the Indian subcontinent, and pointed to the Bowen ratio as a major control on Monsoon precipitation. The interplay between thermodynamic forcing, moisture availability, kinematic forcing from the land-sea breeze circulation, and larger scale dynamics is by no means obvious. For example, clearer skies may imply a greater surface heat flux, a greater land-sea contrast and therefore stronger seabreeze convergence leading to more intense convection over the land, while at the same time implying drier conditions with less moisture available for convection.

Almost every aspect of the thermodynamic and kinematic forcing and moisture availability changes with the propagation of tropical waves, as well as the background wind. For example, it is well recognised that both the diurnal precipitation cycle and the sea-breeze circulation change with the propagation of the Madden-Julian Oscillation (MJO) [4, 5, 6, 7, 8]. Several theories have been invoked to explain these changes. Birch et al. [8] argued that enhanced land-sea breeze circulation arising from strong surface insolation ahead of the MJO led to the increased diurnal precipitation, while Short et al. [4] argued that the changing background winds with the MJO also played a pivotal role in modulating land-sea breeze circulations, thereby modulating the convection. Peatman et al. [6] attributed enhanced precipitation ahead of the MJO to destabilisation of the atmosphere due to surface insolation and low thermal inertia of the land, together with enhanced surface convergence and moisture convergence associated with Kelvin wave propagation. These theories have been tested using gridded observational datasets, and simulated datasets on a variety of scales, but the precise link between thermodynamic forcing at the surface, moisture availability and the diurnal precipitation cycle has not been elucidated. This is largely because testing the hypothesis that radiative forcing at the surface plays an important role in modulating the diurnal precipitation cycle (either through destabilisation or enhanced local flows) requires data that traverses a wide range of spatial and temporal scales.

The diurnal precipitation cycle can also be understood in terms of the changes in cloud properties with the passage of tropical disturbances. [9] used Tropical Rainfall Measuring Mission (TRMM) precipitation estimates and weather states from the International Satellite Cloud Climatology Project (ISCCP) to show that deep and organised convective clouds tended to reach a maximum over land in the enhanced phases of the MJO while scattered or isolated convection reached a maximum in the decreasing of suppressed phases. Interestingly, a similar result was found for Kelvin waves and Equatorial Rossby Waves, indicating that these disturbances behave similarly on a local scale.

The question of the interplay between surface forcing and the diurnal precipitation cycle is important, because numerous studies have shown that atmospheric models on all scales struggle to represent the diurnal precipitation cycle in the Maritime Continent. There are documented errors in the timing and amplitude of the simulated daily peak precipitation, as well as in mean precipitation and land-sea contrast [10, 11, 5, 8, 12]. These errors likely come from a

range of sources, including the cloud microphysics, the turbulence scheme, the radiation scheme and in a larger-scale model, the cumulus parametrisation. For example, Betts and Jakob [13] analysed the tropical diurnal cycle and heat fluxes in the European Centre for Medium-Range Weather Forecasts (ECMWF) model with T319 truncation, and showed that the early initiation of the diurnally forced precipitation could be related to the rapid growth of the cumulus layer as soon as the nocturnal boundary layer was eroded 2 hours after sunrise. They attributed this to the cumulus scheme in the model, but the problem of a diurnal cycle that initiates at the wrong time and too vigorously in the tropics has been observed in almost all scales of weather and climate models (eg. Vincent and Lane [5]). Birch et al. [8] analysed the diurnal precipitation cycle in 10-years of simulations over Sumatra with the UK Unified model with 12 km and 4.5 km grid-lengths, and attributed model errors to the cumulus scheme in the 12 km version and a delay in development of strong updrafts in the 4.5 km version.

The role of daytime surface heating in modulating the diurnal cycle of tropical deep convection has also been considered as means to test model physics in larger-scale models. For example, [14] used in-situ surface flux observations to examine changes to a parameter related to the cumulus adjustment time in a General Circulation Model (GCM). More recently, [15] examined the relationship between the equilibrium climate sensitivity and the diurnal precipitation phase over the ocean, and suggested one hypothesis for this relationship to be related to different impact of cloud radiative effects and different times of day. These larger-scale studies indicate that that the relationship between clouds, fluxes and precipitation have both a non-local and possible up-scale impact.

In this study, we invoke multi-year radiative flux measurements at three locations in Maritime Continent Forests with half-hourly or hourly temporal resolution to interrogate the hypothesis that cloud-free, sunny conditions can enhance the diurnal precipitation cycle, under the right moisture conditions. The relationships between radiative fluxes at the surface, surface relative humidity and afternoon precipitation in a 10-year regional climate model simulation over the Maritime continent is compared with analogous observed relationships. We do not attempt to decompose the results into the indirect and direct effects of kinematic forcing from radiative influences on local flows and effects of warming and/or drying of surface parcels, respectively.

In section 2, the datasets and methods used in the study are introduced. In section 3, we present a self-organising maps decomposition of diurnal patterns in incoming shortwave radiation at the surface, and relate these patterns to precipitation frequency and intensity. Indices of diurnal precipitation are related to local and background moisture in both observed and simulated data, and differences between observed and simulated results are examined in a case-study day of strong diurnally forced convection. Discussion and conclusions are given in sections 4 and 5.

2 | DATA AND METHODS

2.1 | Flux tower measurements

Flux tower measurements were sourced from the ASIA-flux database at three sites in the Maritime Continent (Fig. 1). The ASIA-flux network, part of the FLUXNET program, has been widely used in forest ecosystem exchange studies, carbon and water flux studies and hydrology (see Kang and Cho [16] for a review). Of the three sites used in this study, one is located on the Malay Peninsular (Pasoh Forest Reserve, PSO), and the other two sites are located on the Island of Borneo, Indonesia (Palangkaraya Drained Forest site, PDF and Bukit Soeharto, BKS). The data availability for the three sites is shown in table 1. A few studies have used the network to link atmospheric processes with the surface. For example, Gerken et al. [17] use the global FLUXNET dataset to examine the surface-atmosphere coupling between sensible and latent heat flux and precipitation. Notably, their study illustrates the sparsity of data in the Maritime

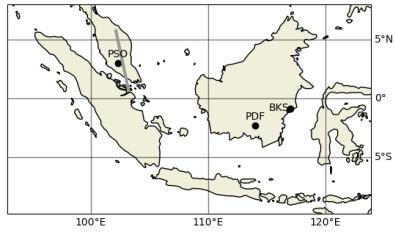

FIGURE 1 Map showing location of the three Asia-Flux measurement towers, and the Cloudsat swath analysed in section 3.5

Continent, with only two of the 251 global sites used in their study located in the region.

2.2 | Convection permitting model simulations

Convection permitting model simulations were sourced from the 10-year Austral summer regional climate simulation over the Maritime Continent [18]. The simulations are run using the WRF model version 3.5 with a horizontal grid spacing of 4 km, and cover from the Austral summers of 2005/2006 to 2014/2015. The domain extends from the eastern Indian Ocean to the Western Pacific Ocean, covering an area of 6564×2136 km^2, with 1641×534 grid points, and is thus expected to capture a broad range of scales of variability and their interactions. The regional model is nested in the ERA Interim Reanalysis (ERAI) [19], with nudging towards ERAI for wavelengths longer than 1000 km. Details of the simulations can be found in Vincent and Lane [5]. Four further simulations for the single case-study presented in section 3.5 were run using a similar setup to that in Vincent and Lane [5], but over a limited domain, without nudging, and using the Thompson, Morrison, WSM6 and WDM6 microphysics schemes respectively.

TABLE 1 Measurement heights and data availability at BKS, PDF and PSO. At site PSO, the relative humidity was calculated from measurements of vapour pressure deficit and temperature.

	BKS		PDF		PSO	
	20010101-20021223		20020101-20051223		20030101-20101223	
	30 min Resolution		1 hr Resolution		1 hr Resolution	
Measurement	Missing [%]	Height [m]	Missing [%]	Height [m]	Missing [%]	Height [m]
SWDOWN	0	30	0	40.6	0.03	52
Sensible HF	59.9	15	42	41.3	20	54
Latent HF	60.8	15	44	41.3	20	54
Precipitation	0	surface	0	41	0.03	53
RH	3.4	15	1.7	41.7	0.03	53

2.3 | Satellite precipitation and cloud observations

ERA-5 reanalysis [20] data was used to calculate the column relative humidity in the vicinity of the observation sites. In section 3.4, satellite precipitation estimates from Tropical Rainfall Mesauring Mission [21] and Joyce et al. [22] were used, together with Radar Reflectivities from the CLOUDSAT cloud profiling radar (95GHz) [23] sourced from `http://www.cloudsat.cira.colostate.edu/data-products/level-2b/2b-geoprof?term=87` [24].

2.4 | Self-organising maps decomposition of incoming shortwave radiation patterns

A self-organising maps (SOM) decomposition was applied to the daily time series of incoming shortwave radiation, where each 24 hour period is considered an input vector. Four SOM nodes were used, since using a greater number led to nodes that appeared qualitatively very similar. SOMs were trained with 10000 iterations, and the results were not sensitive to re-training the SOM array. For each site, the four nodes could be physically related to: a very cloudy day with low insolation all day, a moderately cloudy day, a sunny morning and cloudy afternoon, and a day with almost clear skies. The SOM categories were used to conditionally average sensible and latent heat fluxes and to calculate the diurnal cycles of precipitation frequency and intensity.

2.5 | Diurnal precipitation indices

subsectionindices To examine the response of the diurnal cycle to local forcing and background moisture, three indices of diurnal precipitation are defined (table 2), where LST refers to Local Solar Time. While all days in the study period were used to define the SOM nodes, only days with more than 5 mm of precipitation in the period 1100-2400 LST were considered in the analysis of the diurnal cycle response to local forcing and background moisture.

The diurnal precipitation indices in table 2 were related to the incoming shortwave radiation integrated from sunrise until 1100 LST, the near-surface relative humidity at 1100 LST, and the daily column relative humidity over a 120×120 km box surrounding the site (table 3). The diurnal precipitation indices and the local and non-local forcing indices were compared via scatterplots, correlations and contingency tables.

TABLE 2 Definition of diurnal precipitation indices

Index	Definition
RMAX	Maximum hourly precipitation-rate between 1100 and 2400 LST [mm]
RTOTAL	Total precipitation between 1100 and 2400 LST [mm]
RMAXT	Time of maximum afternoon precipitation

TABLE 3 Definition of local forcing and background moisture indices

Index	Definition
SW00–11	Integrated surface shortwave radiation before 1100 LST
RH11	Surface relative humidity at 1100 LST
RHCOL	Daily column relative humidity over a 120 × 120 km box surrounding the site, from ERA-5

3 | RESULTS

3.1 | Conditionally averaged diurnally averaged precipitation by incoming shortwave radiation

Figure 2 shows the four nodes of the SOM decomposition of incoming shortwave radiation for each of the three stations, together with the frequency and average intensity of precipitation for the days falling into each node. In each case, the nodes have been ordered by SWDOWN, integrated from midnight until 1100 LST. The analysis used all available data for each site, which is 7 years for PSO, 3 years for PDF and 2 years for BKS. The analysis periods do not overlap, which means that these results may be influenced by interannual variability. While this may influence the proportion of days falling into each category, we assume that it does not influence the definition of the categories themselves.

The three sites have several features in common: There is little diurnal variability in precipitation frequency or intensity in Node 1. Nodes 3 and 4 are dominated by the diurnal cycle. In node 3, the second sunniest node, the diurnally forced precipitation begins at around 1200-1500 local time. In node 4, the sunniest node, the precipitation begins later, with a peak in frequency and intensity after 1800 local time at PDF and PSO, and almost no precipitation in the first part of the day. Although the intensity is similar, afternoon precipitation is relatively uncommon, with frequency of precipitation between 0-5%. At all sites, the highest intensity precipitation occurs in node 3. This is the node characterised by a sunny morning and reduced solar insolation in the afternoon.

Node 2 has the most ambiguous precipitation patterns. At PSO, the node 2 precipitation appears to be mostly diurnally forced, while at PDF, there is little diurnal component to the precipitation. At BKS, which has the lowest data availability, there is an interesting peak in precipitation frequency at around midday, which is also reflected in a local minimum in incoming shortwave radiation. It is unclear whether this is coupled to the morning surface forcing, since it is earlier in the day that the precipitation peaks in nodes 3 and 4, and conditions are generally cloudy. Given that BKS is a coastal site, it is possible that this is a non-local diurnal effect, for example relating to interactions with neighbouring islands.

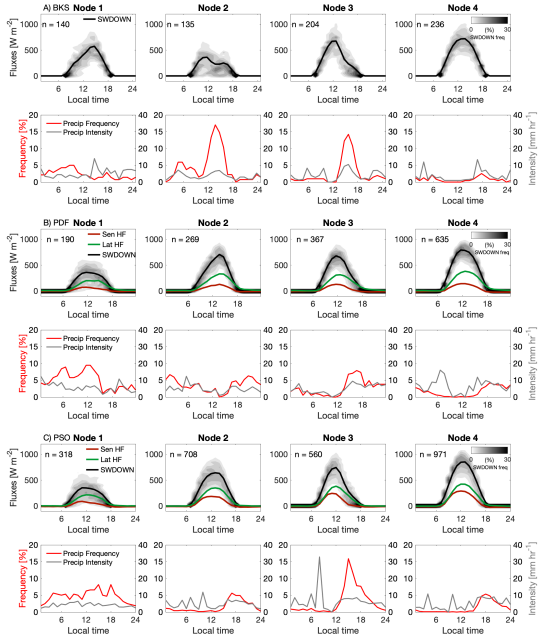

FIGURE 2 Self Organising Maps decomposition of diurnal variations in incoming shortwave radiation (black) and node-averaged surface sensible (dark red) and latent (green) heat flux. Red and grey curves are frequency and intensity of precipitation. Grey contours show the distribution of incoming shortwave radiation about the node mean. A) BKS, B) PDF, C) PSO. The number of days (n) in each node is indicated on the figure.

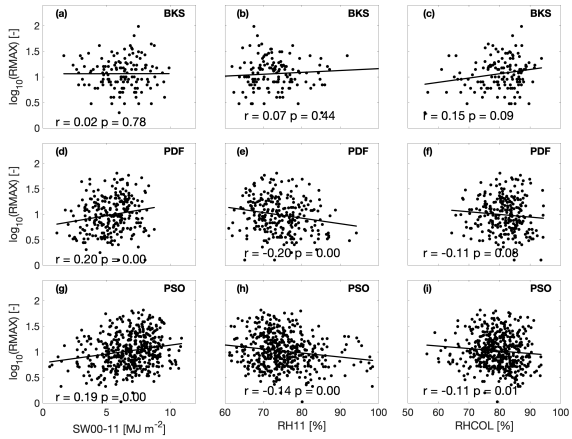

FIGURE 3 Scatter plots of log(RMAX) against SWDOWN, RH11 and RHCOL for BKS (a,b,c), PDF (d,e, f) and PSO (g,h,i)

3.2 | Relationship between diurnal precipitation indices, local forcing and large-scale moisture

Figure 3 shows the relationships between RMAX and SW00–11, RH11 and RHCOL. These results suggest a weak but statistically significant positive relationship between RMAX and SW00-11, and a weak but statistically significant negative relationship between RMAX and RH11 at PDF and PSO (the two inland sites), but almost no correlation at BKS (the coastal site). This may indicate a slightly higher afternoon precipitation peak under sunnier, drier morning conditions at the two inland sites. There is a weak but statistically significant negative relationship between RMAX and RHCOL at PSO, indicating a slight tendency for a lower afternoon precipitation peak under large scale moist conditions, while there is no statistically significant relationship at the other two sites.

For RTOTAL (Fig. 4), these relationships follow similar trends, but the correlation is weaker, the slopes are small and most results are not statistically significant. This implies that considering a single point, the local moisture and surface forcing, as well as the background column moisture, adjust the temporal distribution of precipitation through the afternoon more than the total amount.

Figure 5 shows the relationships between the timing of the afternoon precipitation peak and SW00-11, RH11 and RHCOL. Note that these data fall at discrete hourly intervals. There is little or no relationship between the timing of the afternoon precipitation peak and the local moisture and surface forcing, other than a statistically significant positive relationship between the timing of the afternoon precipitation peak and the RHCOL at BKS, the coastal station. Interestingly, there was also a positive relationship between precipitation amount and RHCOL at this site, significant at the 93% level. Although this site has the least amount of data (2 years), this may indicate a greater influence of the background column moisture at the coastal site relative to the inland sites.

The results in figures 3, 4 and 5 are summarised in figure 6 for site PSO, which shows the joint distribution of SW00-11 and RH11, and SW00–11 and RHCOL, together with the average values of RMAX, RTOTAL and RMAXT for each bin in the joint distribution. These results indicate the heavier values of RMAX in the bins on the sunniest

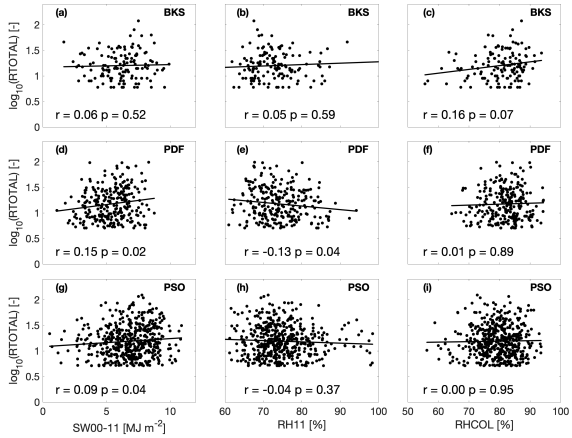

FIGURE 4 As for figure 3, but for log(RTOTAL)

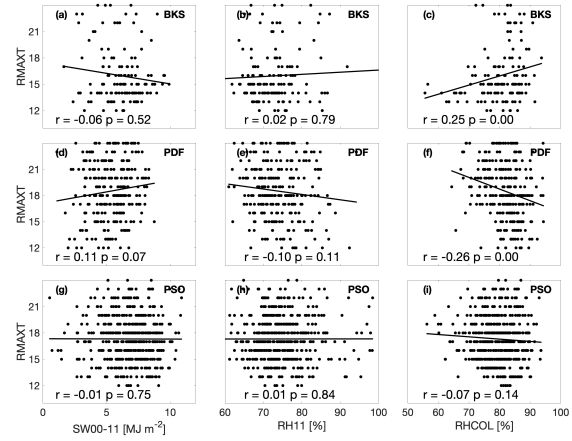

FIGURE 5 As for figure 3 but for RMAXT

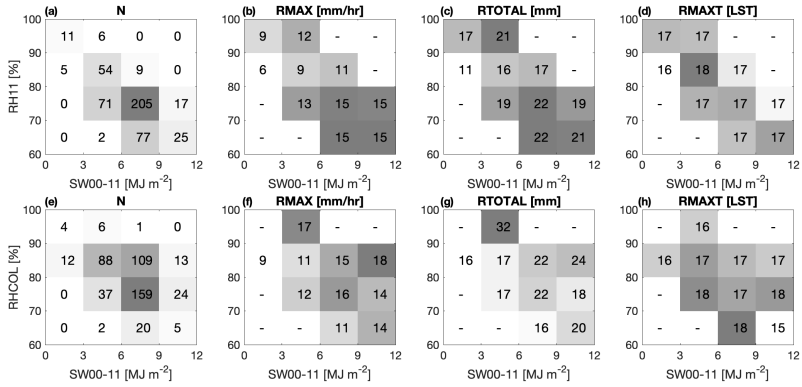

FIGURE 6 Joint distributions (number of occurrences) of SW00–11 and RH11 (a) and SW00–11 and RHCOL (e) at site PSO, and average values of RMAX (b,f), RTOTAL (c,g) and RMAXT (d,h) for each contingency for identified diurnal cycle days. Only averages where there are at least 5 cases are included.

(SW00-11), driest mornings (RH11), while this trend is less clear for the background moisture (RHCOL). The total afternoon precipitation is less clearly associated with the driest, sunniest bins, and we see almost no variation in RMAXT across the distribution.

3.3 | Relationship to intraseasonal scale variability

The changing solar insolation at the surface as a result of variation in the large-scale cloudiness has been proposed as a partial explanation for the changes in the diurnal precipitation cycle with intraseasonal variability. While the results in section 3.2 indicate a tendency for a heavier afternoon precipitation peak under locally sunnier conditions, does this explain the variation in the diurnal cycle with intraseasonal variablity? In figure 7, the frequency of each category of diurnal variation in SWDOWN (figure 2) in each active phase of the MJO (days where the amplitude of the WH04 index > 1) is shown. The significance of changes in the distribution of MJO phases with SW00-11 is tested by sampling, with replacement, from the marginal distributions assuming independence. The marginal distribution is sampled 10000 times. We then compare the actual frequency of occurrence with the distribution of frequencies in the 10000 samples, and assign statistical significance if the actual frequency falls above or below two standard deviations the mean of the sampled distribution. Statistically significant bars in the distributions are indicated in red. For each site, the frequency of days in a given MJO phase adds up to 100% over the four SOM nodes. Although most of the contingencies are not statistically significant according to our null hypothesis, they vary smoothly with WH04 phase which suggests a robust

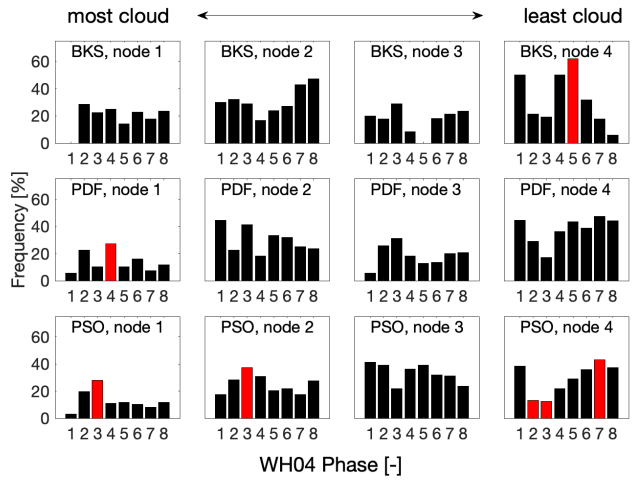

FIGURE 7 Joint distribution of WH04 phase and SOM node for BKS, PDF and PSO sites. Statistical significance is indicated by red bars.

association.

We also note that there are only around 3, 18 and 31 MJO events at BKS, PDF and PSO respectively, where an MJO event is identified as a sequence of days that progress through at least through four WH04 phases, starting no later than phase 2, with at least 10 days with the WH04 amplitude > 1. To be considered an event, each day in the sequence must either stay in the same phase, progress to one of the next two phases or go back by at most one phase. This means that the BKS results are much less robust than the results for PDF and PSO.

At PSO, there is a peak in the cloudiest days (node 1) in WH04 phases 2 and 3, and a peak in the second cloudiest days (node 2) in WH04 phases 2, 3 and 4. Conversely, there is a minimum in the occurrence of the two sunnier nodes in phase 3 (node 3) and in phases 3 and 4 (node 4). This is consistent with the conceptual model of enhanced solar insolation before and after the MJO active phase, and suppressed solar insolation (leading to a suppressed diurnal cycle) during the active phase. Moreover, we see a peak in the sunniest node (4) and relatively rare occurrence of the cloudiest nodes (1 and 2) in MJO phase 7.

The variation in frequency of the nodes is less clear at BKS and PDF, which is likely partly due to the shorter datasets used at these two sites, with the only statistical significance being phase 4 in node 1 (PDF) and phase 5 in node 4 (BKS). However, we do see an increased occurrence of the cloudy nodes in the early phases of the MJO, and an increase in occurrence of the sunny nodes in the later phases. Note that at BKS, nodes 2 and 3 are similar. Fig 7 suggests that these nodes might be reversed in terms of their variation with the MJO, with a greater prevalence of node 3 in phases 2 and 3. This highlights the interface between the local and large-scale variation in cloudiness, although the results presented here show that the cloudiest days may not be the rainiest days.

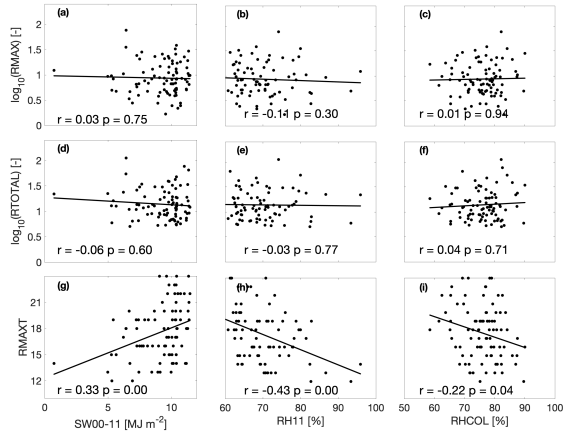

FIGURE 8 Scatter plots of log(RMAX), log(RTOTAL) and RMAXT against SW00–11, RH11 and RHCOL at PSO site from WRF simulations.

3.4 | Comparison with convection permitting model results

The relationships between radiative forcing at the surface, clouds, moisture, convection and precipitation feed into the challenges in simulating the diurnally varying precipitation in the tropics, along with other documented factors such as propagating squall lines associated with diurnally varying gravity waves and the seabreeze circulation. Here, we interrogate the flux-moisture-convection relationships in a 10-year mesoscale Weather Research and Forecasting (WRF) model simulation run with a horizontal grid-length of 4km. Previous validation of the precipitation in these simulations suggested a diurnal cycle that was several hours too early in the day and too intense [5].

Fig. 8 shows the equivalent scatter plots to those in figs. 3–5, but for the WRF model simuations. The data was taken from the nearest grid-point to the PSO station. The time period of the simulations (2006-2015) does not correspond to the time period of the observations (2003-2009), so there may be a minor impact of interannual difference implicit in this analysis. For equivalence to the observations, only the first 7 years of the simulated data was used in this analysis. These results show that there is no obvious relationship between RMAX and RTOTAL and any of SW0–11, RH11 or RHCOL, suggesting that this part of the model response to intraseasonal variability is largely absent. SW00–11 is notably clustered around higher values in the model than the observations, while RH11 is clustered around lower values.

There is an apparent statistically significant relationship between the timing of the simulated diurnal precipitation cycle and all three of SW00–11, RH11 and RHCOL, with sunnier mornings leading to a later precipitation peak, and high values of both morning local moisture and daily background column moisture leading to an earlier peak. This suggests that moisture availability, rather than surface forcing, is modulating the timing of the diurnal precipitation cycle in the simulation.

3.5 | Case study: Sensitivity of the moisture-flux-precipitation relationship to model microphysics

The source of the differences between the observed and simulated coupling between surface forcing, background column moisture and the diurnally varying precipitation is complex. However, we note the low occurrence of cloudy days in the simulations, and hypothesise that either a lack of convective organisation and associated stratiform clouds [25], or a deficiency in low or mid-level cloud may be partly responsible. While these modelling challenges may traverse the radiation, microphysics, surface layer and boundary layer physics in the model, we here choose to examine the sensitivity of the cloudiness and ensuing precipitation to the choice of microphysics scheme.

We examine the model performance on a single day with a strong diurnal component to the diurnal precipitation (20180914). On this day, there was no precipitation before 1500LST, after which there was a total of 41.56 mm in the remainder of the day, with a peak hourly precipitation-rate of 24.48 mm. The day fell into node 3 of the SOM analysis in fig. 2.

This day was chosen as a typical example of diurnally forced precipitation at the PSO site, but also because a CLOUDSAT overpass coincided with the observation location at 0600UTC, or 1300 LST, which is several hours ahead of the start of the observed precipitation. The WRF model version 4.1.1 was run with a horizontal grid length 12 km, with nested domains with grid lengths of 4 km and 1.33 km respectively. No nudging was applied. The results here are for the 1.33 km nest. Four simulations, using the WSM6, WDM6, Morrison and Thompson microphysics scheme were run, starting at 201809131200, giving 18 hours of spin-up time ahead of the CLOUDSAT overpass. The model setup is otherwise identical to that in Vincent and Lane [5].

CLOUDSAT radar reflectivities were produced from the WRF model simulations using the Quickbeam package [26] with default settings for hydrometeor classes. This package has been used to compare simulated clouds from the WRF model previously (eg. Huang et al. [27]). All four microphysics schemes used here have the same 6 classes of hydrometeors, albeit with different definitions of the classes. The Quickbeam settings have been kept constant for the four simulations, which may be responsible for some of the differences seen in the simulated reflectivities. However, there are notable qualitative differences in the observed and simulated reflectivities. The Thompson and Morrison schemes both show a continuous area of stratiform cloud above 10 km, and a distinct layer of lower cloud at around 5 km. In contrast, the WSM6 and WDM6 schemes develop distinct turrets of cloud above 10 km, and a minimal cloud layer at 5 km.

The four model simulations were also compared with the TRMM3B42 [21] and CMORPH [22] satellite precipitation estimates for the same time as the CLOUDSAT scan (Fig. 10). The precipitation-rate is shown both at native resolution and averaged to the resolution of TRMM3B42. When averaged to the native resolution of TRMM3B42 (right hand panels), it is evident that the precipitation in the WRF model is more widespread than in the satellite estimates, and that it is spatially concentrated inland compared to the small regions of coastal precipitation in the satellite precipitation estimates. The most widespread precipitation is associated with the Thompson and Morrison microphysics schemes, which also showed the most dense cloud cover and strongest convective turrets at the same time in the CLOUDSAT reflectivities. In this case study, the diurnally varying precipitation, averaged over all land areas of the domain (Fig. 11) is closest to that observed by TRMM3B42 in the simulations using the WDM6 and WSM6 microphysics schemes. However, on comparing the simulated surface energy balance at PSO with the observations (fig. 12), it is apparent that the different simulations have captured critically different aspects of the diurnal evolution - for example, the Thompson scheme has the sunniest morning conditions, the WSM6 scheme shows the cloudiest conditions in both morning and afternoon (not dissimilar from the observations), and the Morrison scheme shows a brief dip in insolation in the middle of the day. This exemplifies that the diurnal cycle of clouds and precipitation is made up of a combination of processes

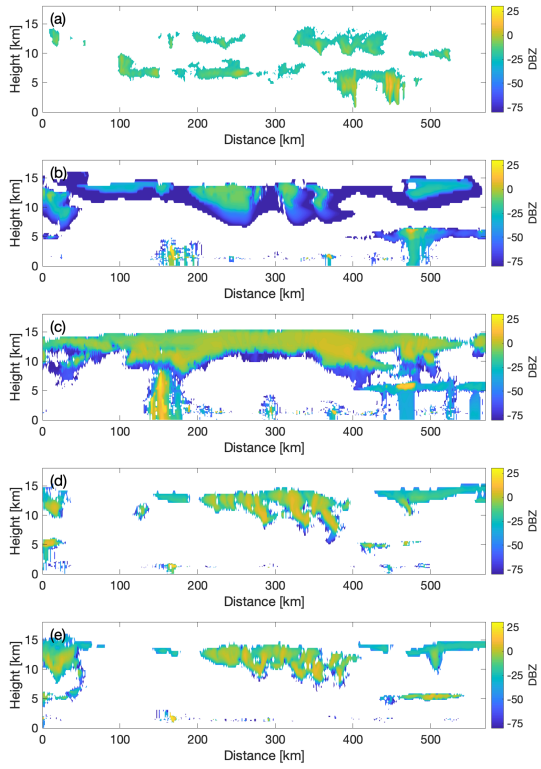

FIGURE 9 (a) Reflectivity from CLOUDSAT, 200809140602 (b) Simulated reflectivity WRF-Thompson, (c) Simulated reflectivity WRF-Morrison (d) Simulated reflectivity WRF-WSM6, (e) Simulated reflectivity WRF-WDM6. Simulations are valid at 200809140600.

and feedbacks, rather than a simple build-up and decay of convection.

4 | DISCUSSION

This study responds to the hypothesis that changes in downwelling shortwave radiation at the surface associated with the MJO play a fundamental role in amplifying or dampening the diurnal precipitation cycle [7, 6, 28, 8]. This question is confounded by the fact that both moisture and surface radiative fluxes change with the MJO, while the background wind field and its interaction with the complex coastlines and topography of the region also varies. Moreover, warming and drying of the surface in periods of higher insolation have an opposite influence on the ensuing moist adiabat. These competing factors, and the heterogeneity of surface conditions in the Maritime Continent, largely explain the challenge of aligning MJO-scale variability with limited geographical areas within the region. For example, when looking at precipitation trends with the MJO over a small spatial area Lestari et al. [29] found minimal connection with MJO-scale variability around Jakarta, or even variability of the reverse sign to what is expected. The nuances in these relationships define the challenge of simulating the diurnal and MJO-scale variability in almost any resolution of model.

The long-term surface flux and precipitation measurements of the Asia-flux network provide an ideal opportunity to unpack the relationship between local moisture, local surface heat fluxes, precipitation and intraseasonal-scale variability, albeit at a limited and likely un-representative selection of locations. In this study, we do not consider the additional complexity that increasing surface heating also increases the land-sea temperature difference, which may then induce a stronger land-sea breeze circulation and therefore more convection assocaited with seabreeze convergence. This is a limitation of the current study, because the result that sunnier mornings sometimes leads to heavier afternoon precipitation may be partly related to shifting surface parcels to a warmer moist adiabat, and partly related to initiation of a stronger land-sea breeze circulation. Both of these effects work in the same direction. However, we note that the clearest results are from the two non-coastal sites (PSO and PDF), while little to no relationships were found for the coastal site, which is assumed to be because it is governed by non-local processes.

Our results suggest that the sunniest days are related to infrequent, heavy diurnally forced precipitation, while the cloudiest days show frequent, lighter precipitation with little diurnal variation. We also show that the sunniest, drier days are associated with a greater likelihood of heavy afternoon precipitation. These results have high statistical significance at two out of the three sites studied. In contrast, there were statistically significant, but very weak relationships between the total amount of afternoon precipitation and the morning incoming shortwave radiation. This is consistent with Grabowski et al. [30] who argued that representation of bulk convection was relatively insensitive to model resolution or whether the model runs in two or three dimensions, but that the diurnal evolution was sensitive to these factors. These results are also consistent with Bretherton et al. [2], who demonstrates a close relationship between column relative humidity (defined as column water vapour path divided by saturated column water vapour path) and precipitation on monthly and daily timescales. That the total afternoon precipitation is relatively insensitive to the surface conditions strongly suggests that this is controlled more by larger scale moisture variations, while the surface acts as a control on the distribution of precipitation during the day.

On relating the data-driven categorisation of days according to their diurnal evolution of incoming short-wave radiation to the MJO-phases of the WH04 index, we find expected trends only in a general sense, with the highest prevalence of cloudy days in the MJO active phases and the highest prevalence of sunny days in the inactive phases. However, few of these relationships are statistically significant, indicating that locally we see a representation of all types of days in all MJO phases.

The feedback between radiative fluxes at the surface and convection is only one piece of the puzzle in realistic

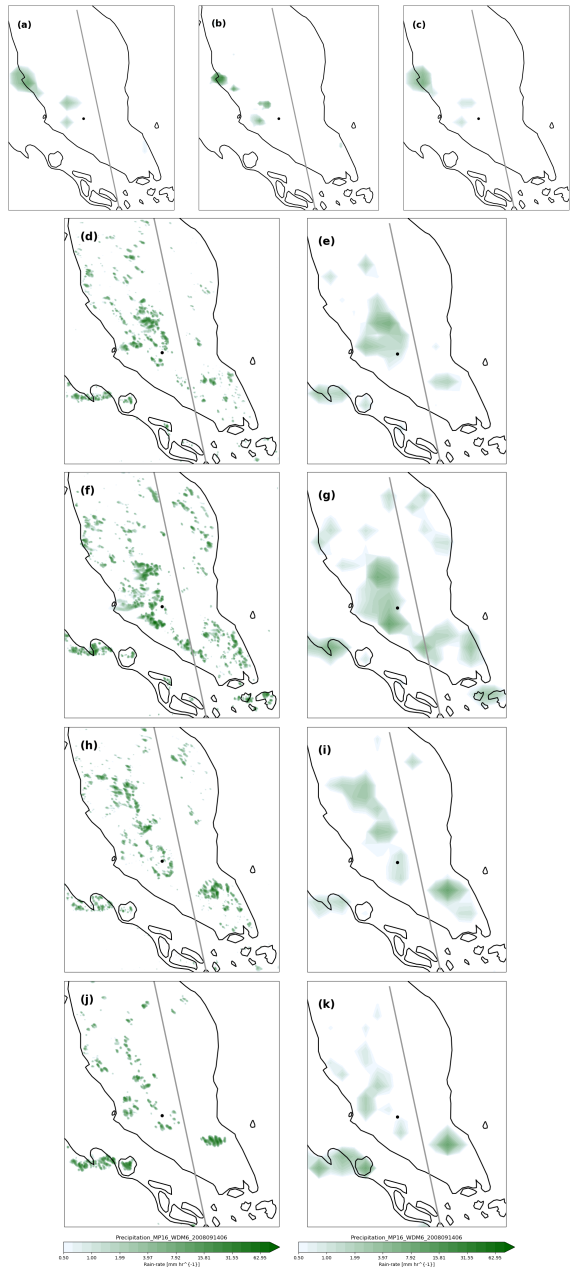

FIGURE 10 Hourly precipitation-rate at 200809140600 UTC from TRMM3B42 (a), CMORPH (b - native resolution,c - TRMM resolution), WRF-Thompson (e,f), WRF-Morrison (g,h), WRF-WSM6 (i,j) and WRF-WDM6 (k,l). Left hand panel shows native resolutions (d,f,h,j) and right hand panel shows data averaged to TRMM resolution (e,g,i,k).

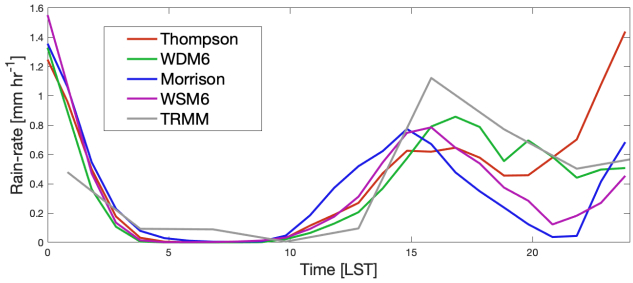

FIGURE 11 Land-area averaged diurnal variation in precipitation from 2008091400 until 2008091500 LST from WRF experiments and TRMM3B42.

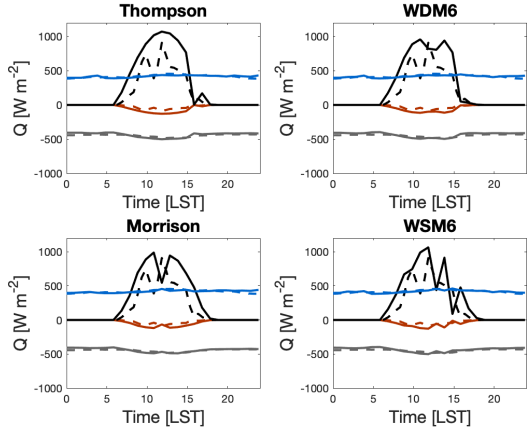

FIGURE 12 Observed (dashed lines) and simulated (solid lines) surface energy balance at PSO. Blue: Longwave down, Black: Shortwave down, Grey: Longwave up, Red: Shortwave up.

simulations of tropical precipitation on a sub-daily scale. The fact that the simulations do not capture the inverse relationship between morning insolation and afternoon precipitation is likely more symptomatic of the fact that these simulations are too sunny overall, meaning that the cloudy days with suppressed insolation are largely missing from this relationship. Other models have been shown to be too cloudy, with diurnally forced precipitation initiating too late in the day [8]. Thus these results do not generalise to all models, but demonstrate that correct relationships between the microphysics, surface and radiation physics are required to accurately simulate diurnally forced precipitation, and none of these can be solved in isolation. The fact that the simulated convection tends to have small, discrete towers of convection that are too vigorous impinges on all these relationships.

The work here also tests the hypothesis that the diurnal cycle responds to convective initiation via surface heat fluxes more than to the enhanced moisture associated with the main envelope of intraseasonal variability. This hypothesis is found to be broadly accurate, with sunnier, drier mornings leading to heavier afternoon precipitation-rates, while no such relationship exists with total afternoon precipitation. However, the scatter in the relationships between surface forcing and afternoon precipitation, and the variations in patterns of solar insolation at the surface with MJO phase shows that this hypothesis only explains one aspect of the variation in diurnal cycle with the MJO. Non-local aspects, such as the land-sea breeze circulation [4], density currents, gravity waves and propagation of diurnally varying squall-line from neighbouring regions [31, 32] all play a role in the multi-scale controls on the diurnal cycle. Notably, these relationships have only been tested at three sites, one of which had insufficient data to demonstrate any statistically significant results. To the best of our knowledge, this is the first study that tests this hypothesis using data that traverses the microscale through to intraseasonal scales. A broader study might be achieved using satellite data and gridded precipitation products, although these relationships are influenced by very small scale processes, and the local influences might be nearly impossible to deduce in this way. Convection-permitting models may capture some aspects of the diurnally varying tropical atmosphere, such as land-sea breeze circulations, but as demonstrated in this study, are unlikely to capture the very local processes, and therefore need to be used with care for processed based studies.

5 | CONCLUSIONS

In this study, we examined local and large-scale moisture controls on the diurnally forced precipitation in the tropics. This work exemplifies the inter-scale nature of the diurnal precipitation cycle in the tropics, from intra-seasonal scales down to turbulent transport of heat and moisture at the surface. The hypothesis that sunnier morning conditions leads to heavier afternoon precipitation was found to be partly correct, but explains only a small part of variation in the intensity of the diurnally forced afternoon precipitation.

We tested the same hypothesis in long dataset of convection-permitting simulations over the region, and found that the observed relationships were non-existent in the simulated data. Moreover, the simulated conditions were shown to be too sunny generally. Although the simulations have been shown in previous studies to capture some aspects of the diurnal precipitation cycle, the results here suggest that the model response to surface forcing is deficient.

Detailed examination of a single day with diurnally forced precipitation reveals a diversity of diurnal and spatial patterns of precipitation and clouds. As one part of the network of processes that control the diurnal precipitation cycle, the feedback between cloudiness, incoming shortwave radiation, surface fluxes and convection is a major source of uncertainty. This study did not consider the inter-related effect of the land-sea breeze circulation and other mesoscale flows on diurnally forced precipitation. These are non-local effects, and since their influence on the diurnal precipitation cycle is likely to have the same sign as the local effects - that is, sunnier conditions leading to a stronger land-sea breeze circulation - it is not possible the extricate these individual influences. A careful idealised modelling study at very high

resolution could help disentangle these influences.

While this study has focused on observations and convection-permitting models, it is clear that neither the local or non-local controls on diurnally forced precipitation will be simulated accurately in a climate-scale model. However, the fact that the total afternoon precipitation was affected less by the surface forcing than the intensity of the diurnal precipitation peak may suggest that on daily and longer time scales, the local forcing is less important.

ACKNOWLEDGEMENTS

Y Huang was supported by the ARC Centre of Excellence for Climate Extremes (CE170100023) and C Vincent was support by the ARC Discovery Project (DP190100786). The authors would like to thank the AsiaFlux network for permission to use their data (http://asiaflux.net/) in this study. Analysis was conducted on the Australian National Computing Infrastructure (NCI)

REFERENCES

[1] Bergemann M, Jakob C. How important is tropospheric humidity for coastal rainfall in the tropics? Geophysical Research Letters 2016;http://arxiv.org/abs/1603.02392.

[2] Bretherton CS, Peters ME, Back LE. Relationships between Water Vapor Path and Precipitation over the Tropical Oceans. Journal of Climate 2004;17:1517–1528.

[3] Thomas L, Malap N, Grabowski WW, Dani K, Prabha TV. Convective environment in pre-monsoon and monsoon conditions over the Indian subcontinent: The impact of surface forcing. Atmospheric Chemistry and Physics 2018;18(10):7473–7488.

[4] Short E, Vincent CL, Lane TP. Diurnal cycle of surface winds in the maritime continent observed through satellite scatterometry. Monthly Weather Review 2019;147(6).

[5] Vincent CL, Lane TP. A 10-year Austral summer climatology of observed and modeled intraseasonal , mesoscale and diurnal variations over the Maritime Continent. Journal of Climate 2017;.

[6] Peatman SC, Matthews AJ, Stevens DP. Propagation of the Madden-Julian Oscillation through the Maritime Continent and scale interaction with the diurnal cycle of precipitation. Quarterly Journal of the Royal Meteorological Society 2014 Apr;140(680):814–825.

[7] Rauniyar SP, Walsh KJE. Scale interaction of the diurnal cycle of rainfall over the MC and australia: influence of the MJO. Journal of Climate 2013;26:1304–1321.

[8] Birch CE, Webster S, Peatman SC, Parker DJ, Matthews AJ, Li Y, et al. Scale interactions between the MJO and the western Maritime Continent. J Clim 2016;.

[9] Worku LY, Mekonnen A, Schreck CJ. The impact of MJO, Kelvin, and equatorial rossby waves on the diurnal cycle over the maritime continent. Atmosphere 2020;11(7):0–9.

[10] Fonseca KTY R, Teo CK. Multi-scale interactions in a high-resolution tropical-belt experiment and observations. Climate Dynamics 2019;52(5-6):3503–3532. http://dx.doi.org/10.1007/s00382-018-4332-y.

[11] Kim H, Lee MI, Cha DH, Lim YK, Putman WM. Improved representation of the diurnal variation of warm season precipitation by an atmospheric general circulation model at a 10 km horizontal resolution. Climate Dynamics 2019;53(11):6523–6542. https://doi.org/10.1007/s00382-019-04943-6.

[12] Ahn MS, Kim D, Kang D, Lee J, Sperber KR, Gleckler PJ, et al. MJO Propagation Across the Maritime Continent: Are CMIP6 Models Better Than CMIP5 Models? Geophysical Research Letters 2020;47(11):1–9.

[13] Betts AK, Jakob C. Evaluation of the diurnal cycle of precipitation, surface thermodynamics, and surface fluxes in the ECMWF model using LBA data. Journal of Geophysical Research: Atmospheres 2002;107(20):LBA 12–1–LBA 12–8.

[14] Lin X, Randall DA, Fowler LD. Diurnal variability of the hydrologic cycle and radiative fluxes: Comparisons between observations and a GCM. Journal of Climate 2000;13(23):4159–4179.

[15] Christopoulos C, Schneider T. Assessing Biases and Climate Implications of the Diurnal Precipitation Cycle in Climate Models. Geophysical Research Letters 2021;48(13):1–9.

[16] Kang M, Cho S. Progress in water and energy flux studies in asia: A review focused on eddy covariance measurements. Journal of Agricultural Meteorology 2021;77(1):2–23.

[17] Gerken T, Ruddell BL, Yu R, Stoy PC, Drewry DT. Robust observations of land-to-atmosphere feedbacks using the information flows of FLUXNET. npj Climate and Atmospheric Science 2019;2(1). http://dx.doi.org/10.1038/s41612-019-0094-4.

[18] Vincent CL, Lane TP, Maritime Continent WRF DJF 4km simulations v1.0. NCI National Research Data Collection; 2016.

[19] Dee DP, Uppala SM, Simmons AJ, Berrisford P, Poli P, Kobayashi S, et al. The ERA-Interim reanalysis: configuration and performance of the data assimilation system. Quarterly Journal of the Royal Meteorological Society 2011;137:553–597.

[20] European Centre for Medium-Range Weather Forecasts, ERA5 Reanalysis. Boulder CO: Research Data Archive at the National Center for Atmospheric Research, Computational and Information Systems Laboratory; 2017. https://doi.org/10.5065/D6X34W69.

[21] Tropical Rainfall Mesauring Mission, TRMM (TMPA) Rainfall Estimate L3 3 hour 0.25 degree x 0.25 degree V7; 2011. https://disc.gsfc.nasa.gov/datacollection/TRMM_3B42_7.html.

[22] Joyce RJ, Janowiak JE, Arkin Pa, Xie P. CMORPH: A Method that Produces Global Precipitation Estimates from Passive Microwave and Infrared Data at High Spatial and Temporal Resolution. Journal of Hydrometeorology 2004;5:487–503.

[23] Im E, Wu C, Durden SL. Cloud profiling radar for the CloudSat mission. IEEE Aerosp Electron Syst Mag 2005;20(10):15–18.

[24] Marchand R, Mace GG, Ackerman T, Stephens G. Hydrometeor detection using Cloudsat - An earth-orbiting 94-GHz cloud radar. Journal of Atmospheric and Oceanic Technology 2008;25(4):519–533.

[25] Vincent CL, Lane TP. Mesoscale Variation in Diabatic Heating around Sumatra , and Its Modulation with the Madden – Julian Oscillation. Monthly Weather Review 2018;146:2599–2614.

[26] Haynes JM, Marchand RT, Luo Z, Bodas-Salcedo A, Stephens GL. A multipurpose radar simulation package: QuickBeam. Bulletin of the American Meteorological Society 2007;88(11):1723–1727.

[27] Huang Y, Siems ST, Manton MJ, Thompson G. An evaluation of WRF simulations of clouds over the southern ocean with a-train observations. Monthly Weather Review 2014;142(2):647–667.

[28] Vincent CL, Lane TP. Evolution of the diurnal precipitation cycle with the passage of a Madden-Julian Oscillation event through the Maritime Continent. Monthly Weather Review 2016;In Press.

[29] Lestari S, King A, Vincent C, Karoly D, Protat A. Seasonal dependence of rainfall extremes in and around Jakarta , Indonesia. Weather and Climate Extremes 2019;24(September 2018):100202. https://doi.org/10.1016/j.wace.2019.100202.

[30] Grabowski WW, Wu X, Moncrieff MW, Hall WD. Cloud-resolving modeling of cloud systems during phase III of GATE. Part II: Effects of resolution and the third spatial dimension. Journal of the Atmospheric Sciences 1998;55(21):3264–3282.

[31] Ruppert JH, Chen X, Zhang F. Convectively forced diurnal gravity waves in the maritime continent. Journal of the Atmospheric Sciences 2020;77(3):1119–1136.

[32] Baranowski DB, Flatau MK, Flatau PJ, Matthews AJ. Phase locking between atmospheric convectively coupled equatorial Kelvin waves and the diurnal cycle of precipitation over the Maritime Continent. Geophysical Research Letters 2016;43(15):8269–8276.

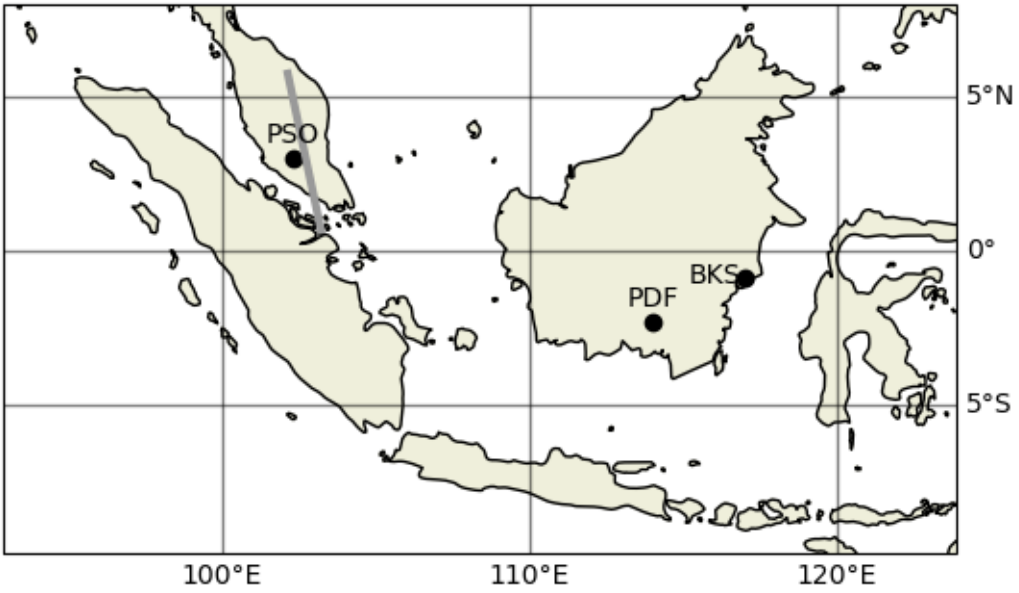

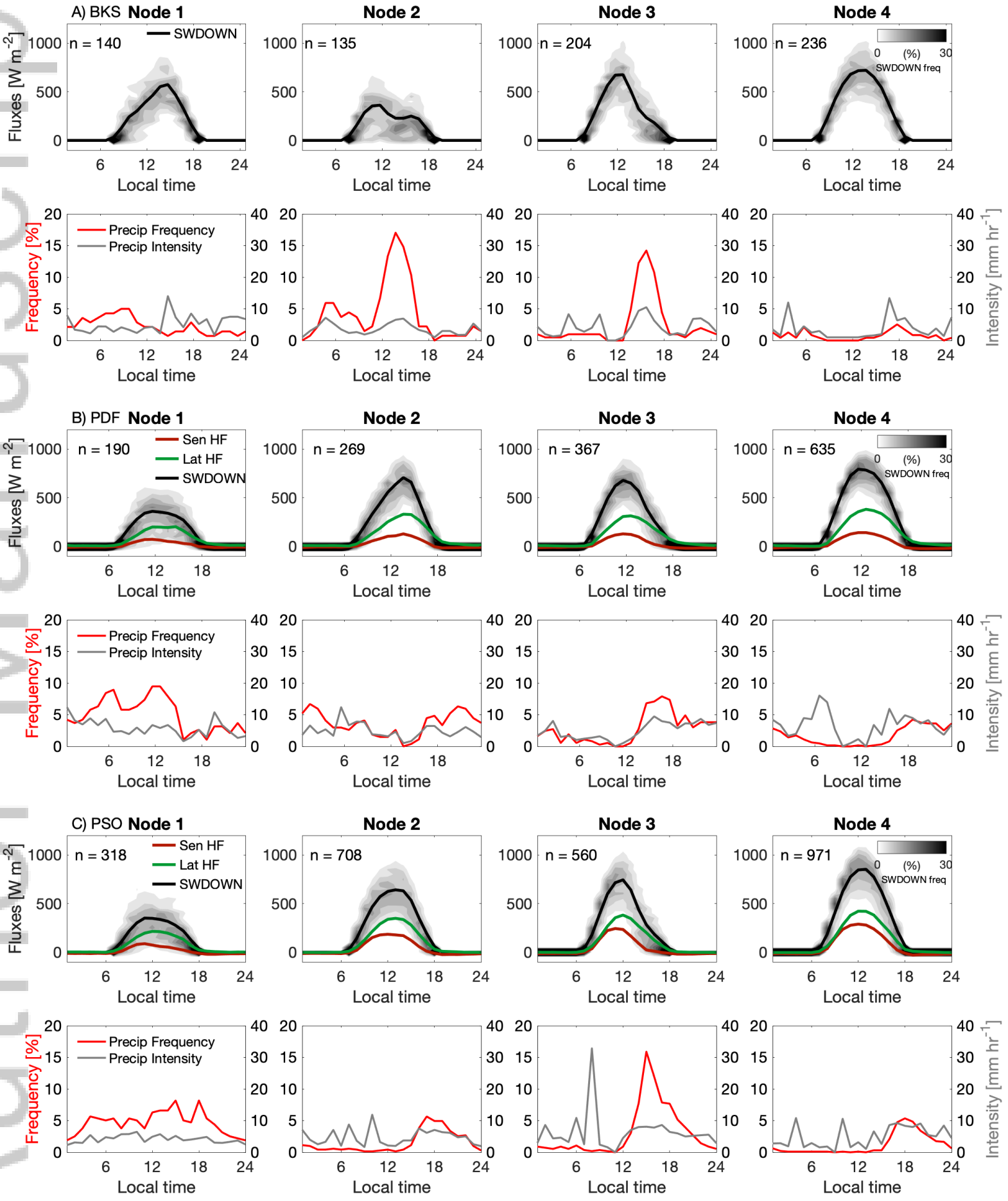

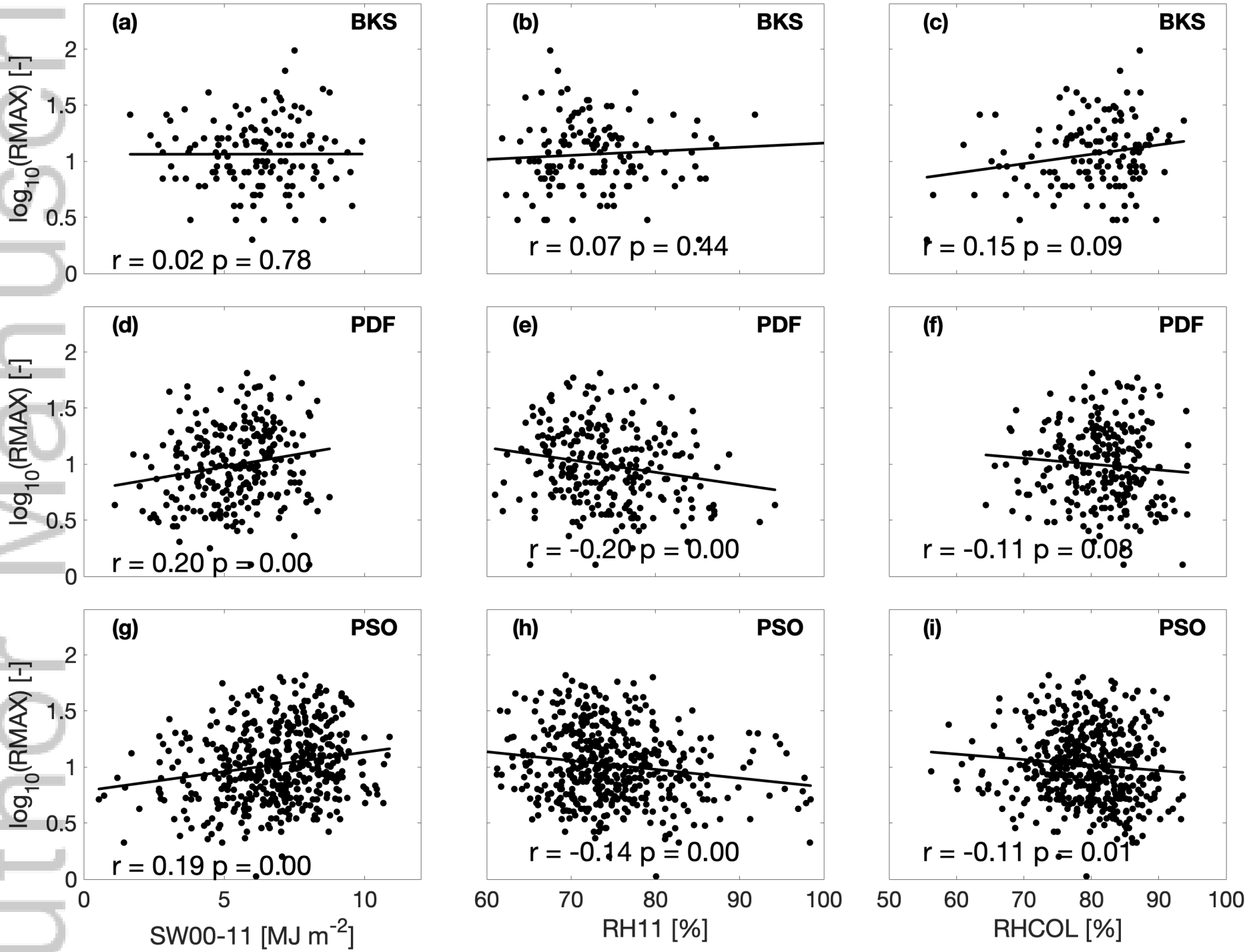

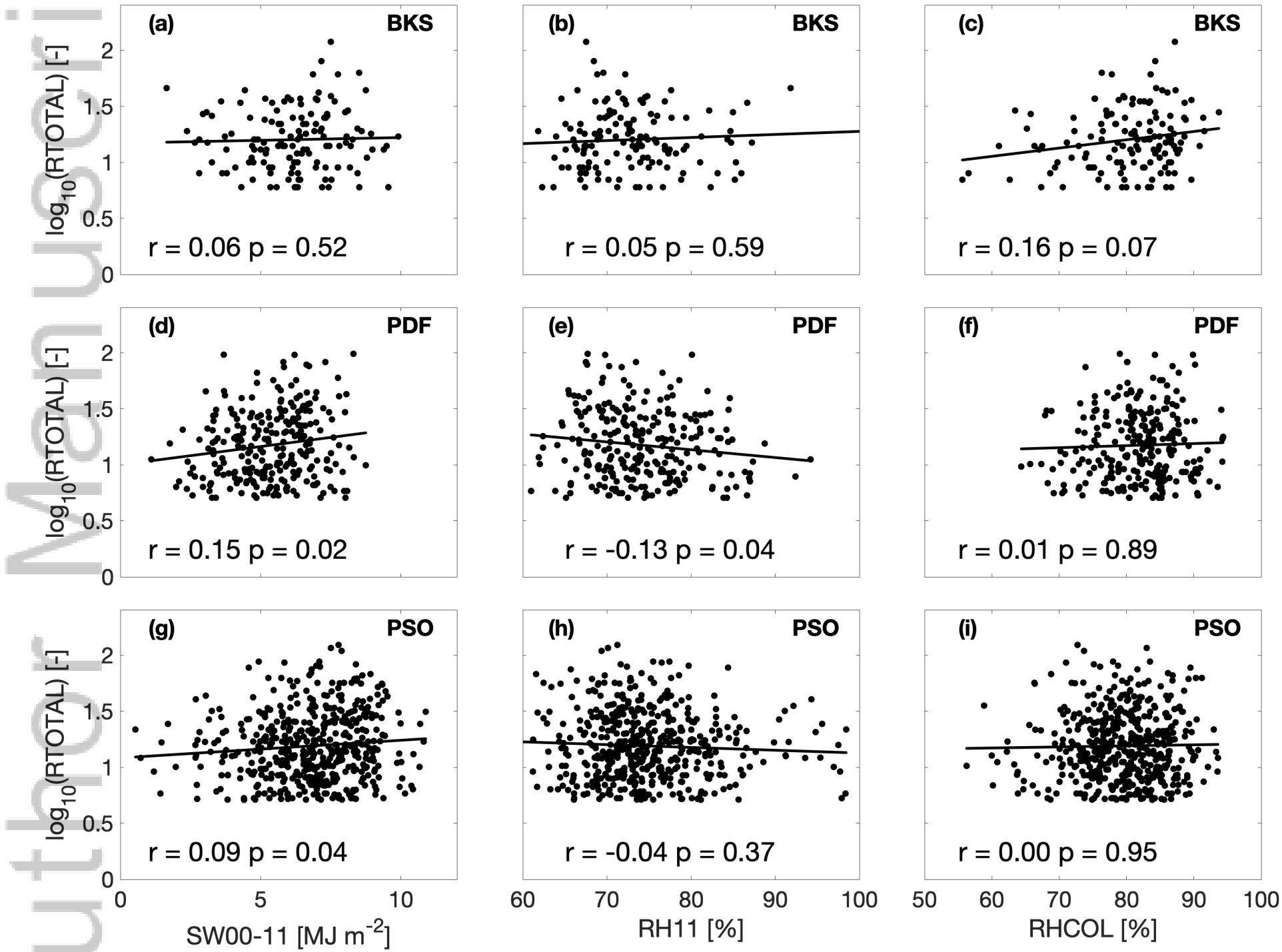

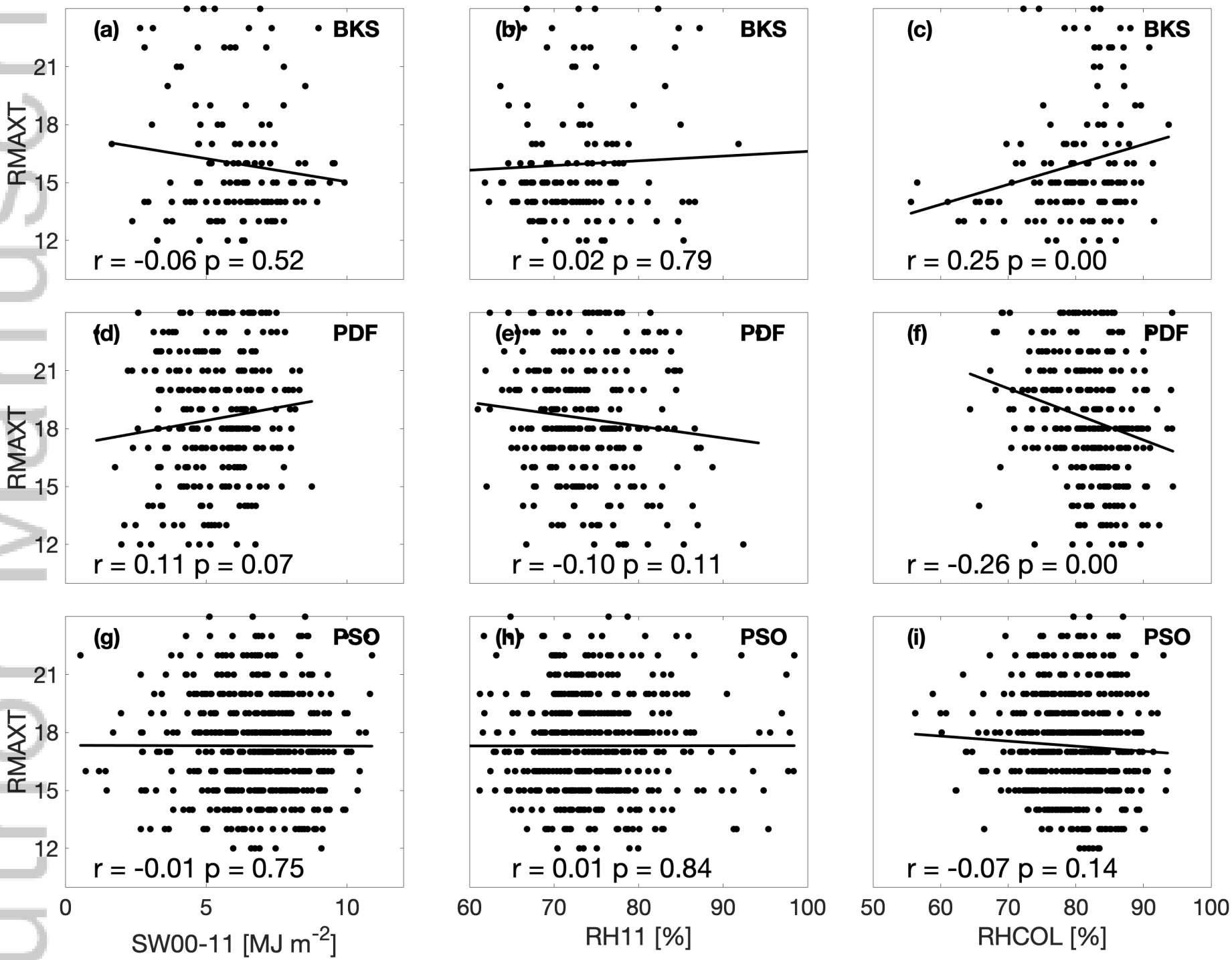

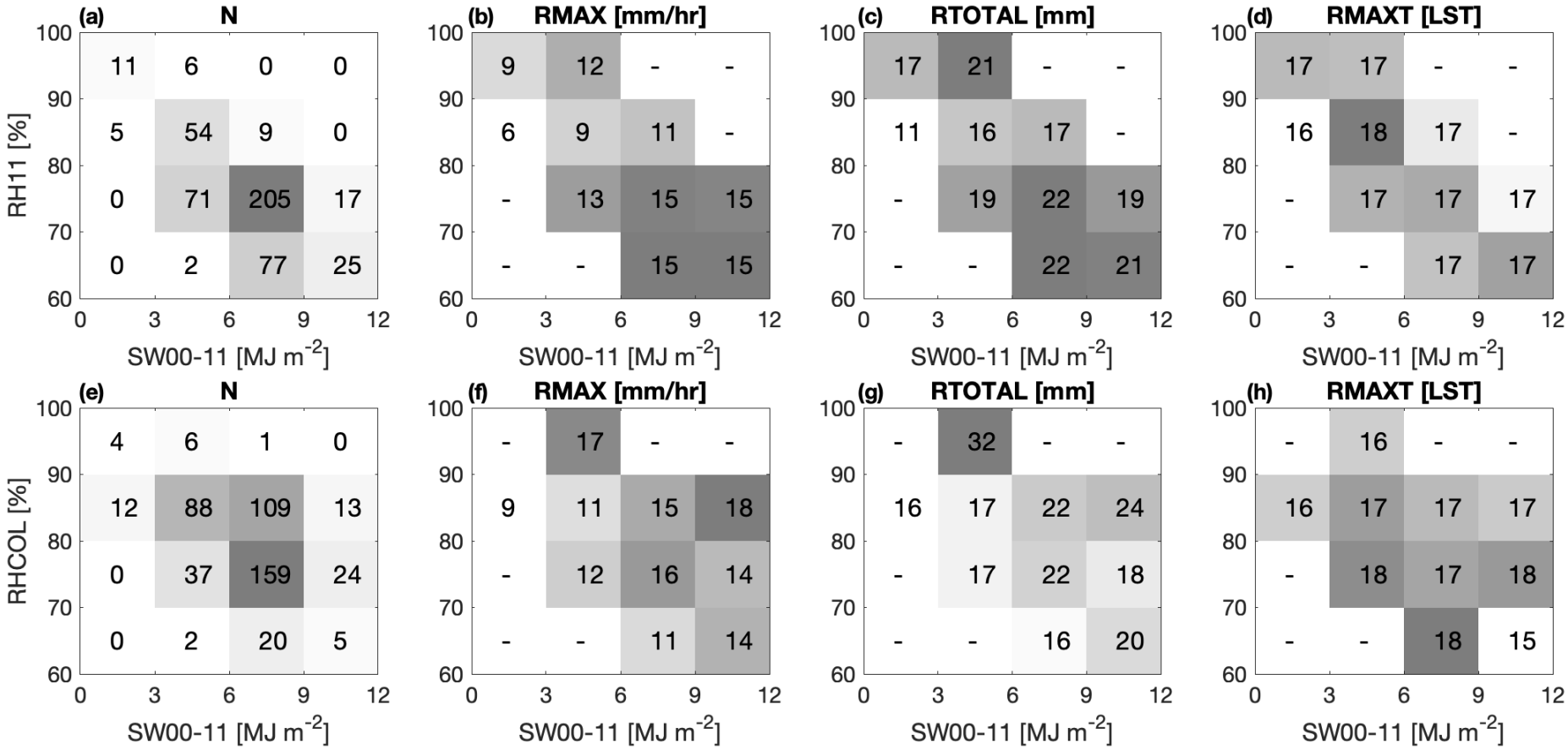

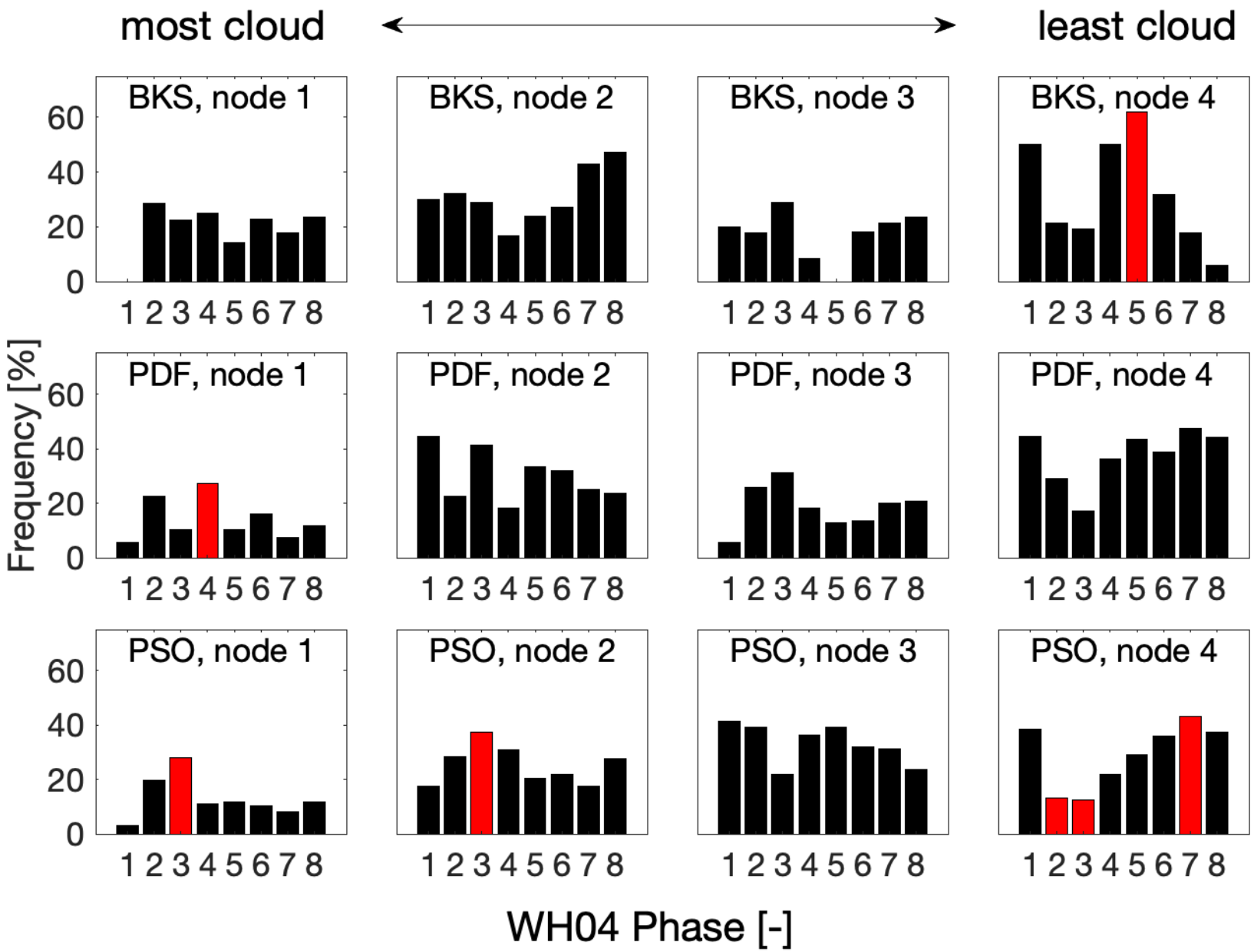

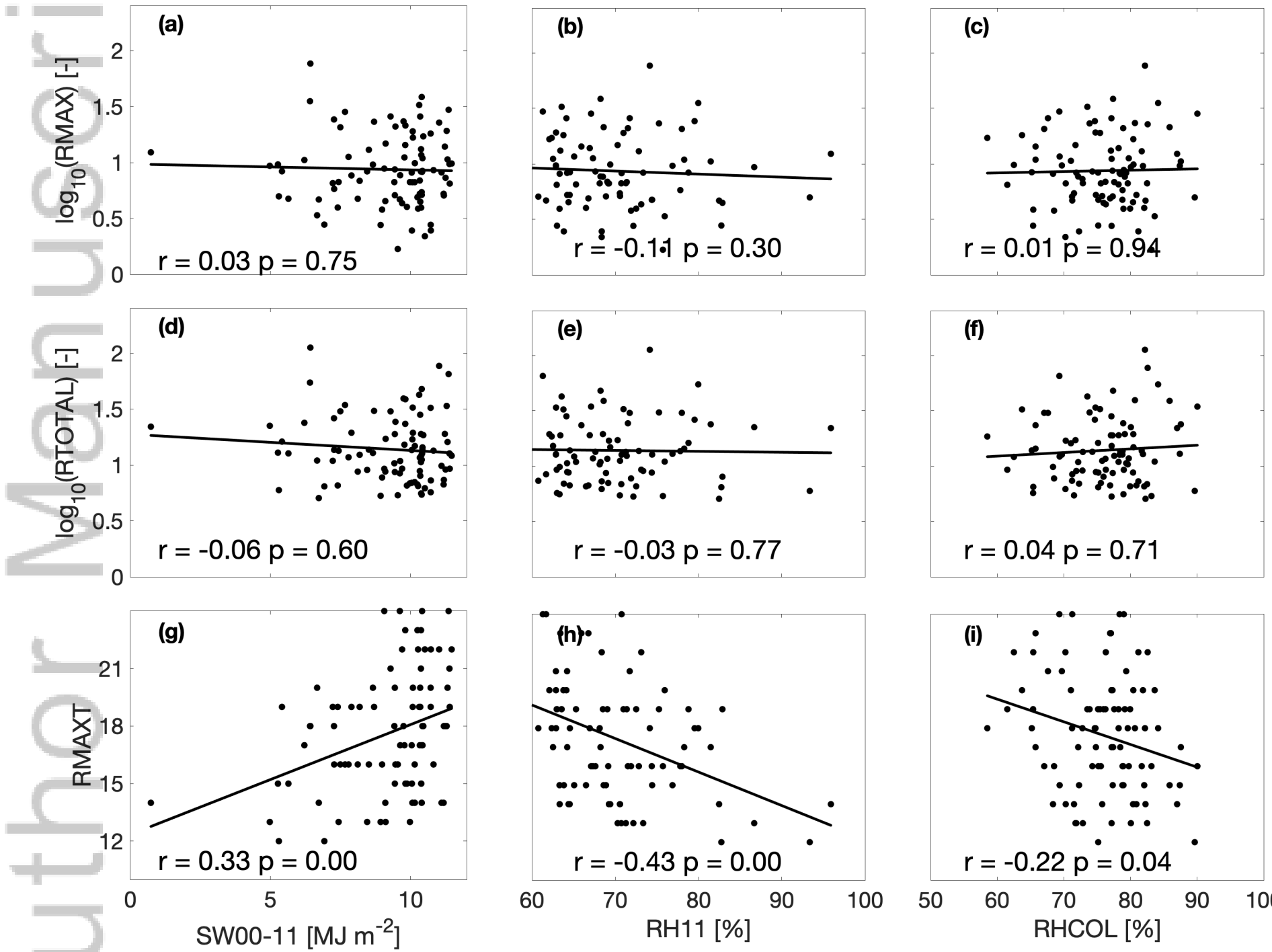

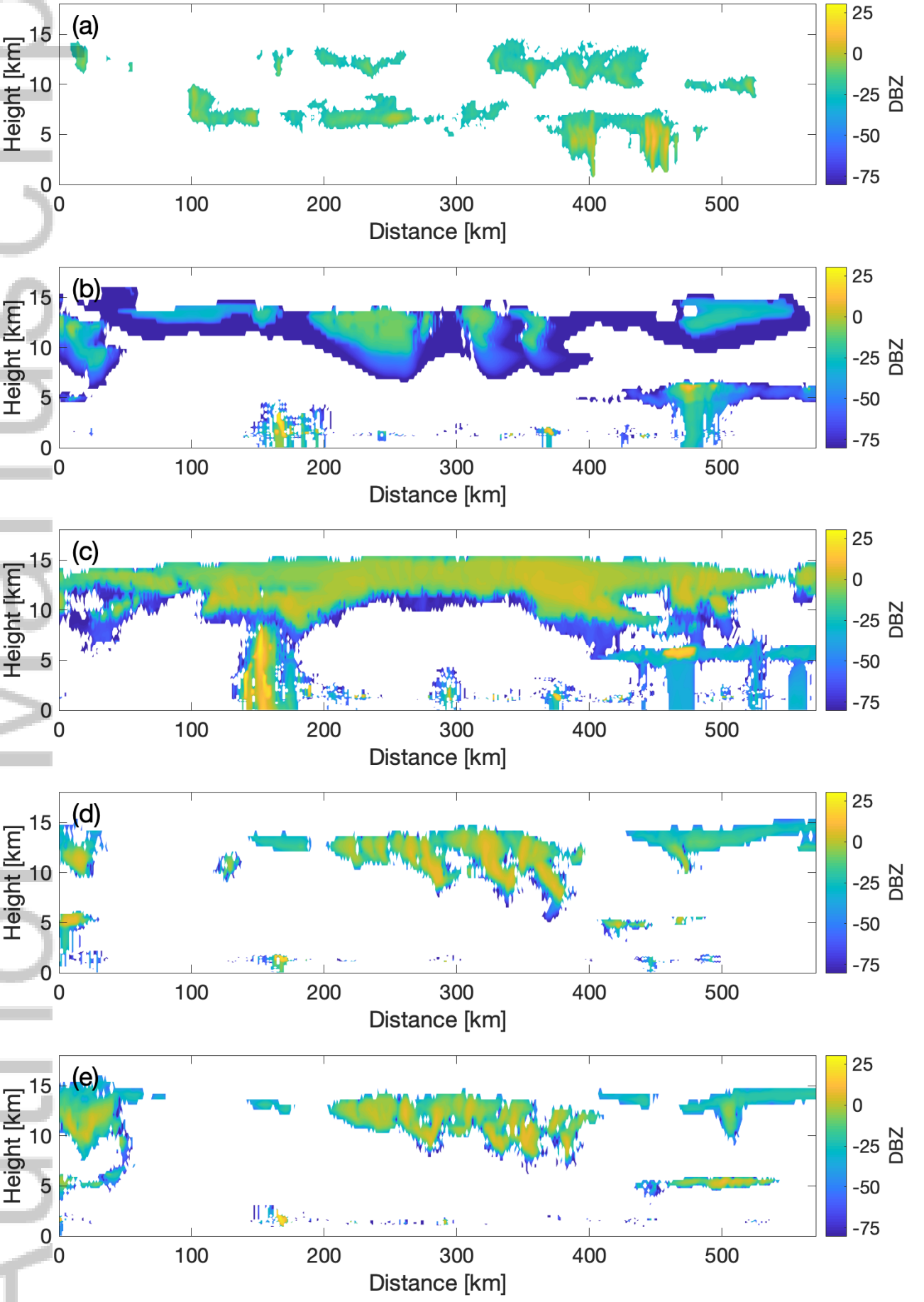

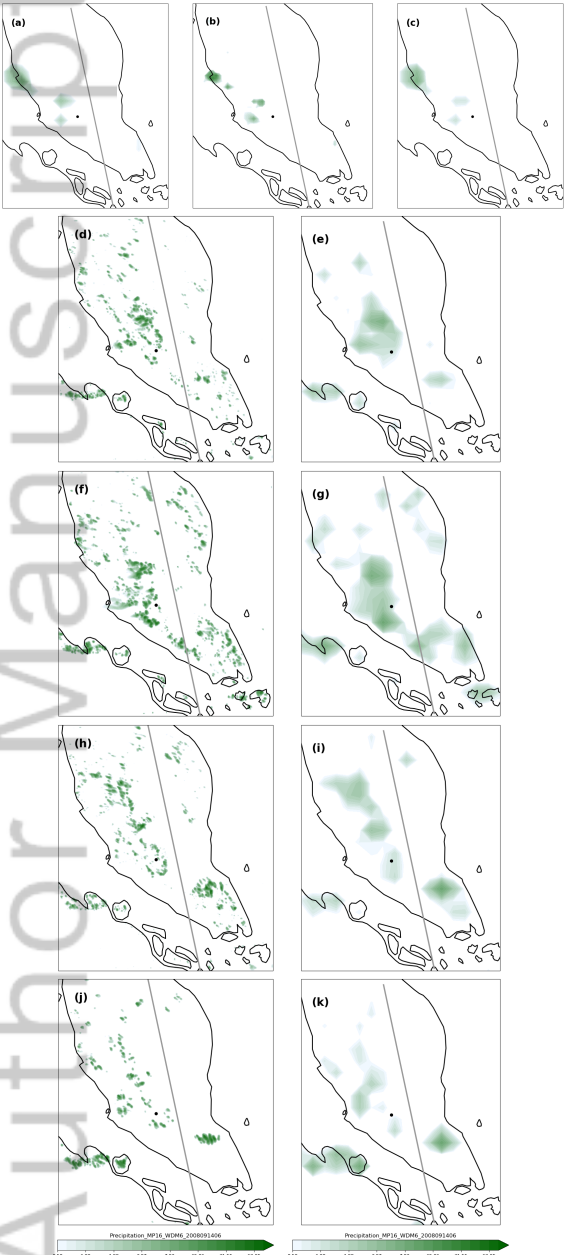

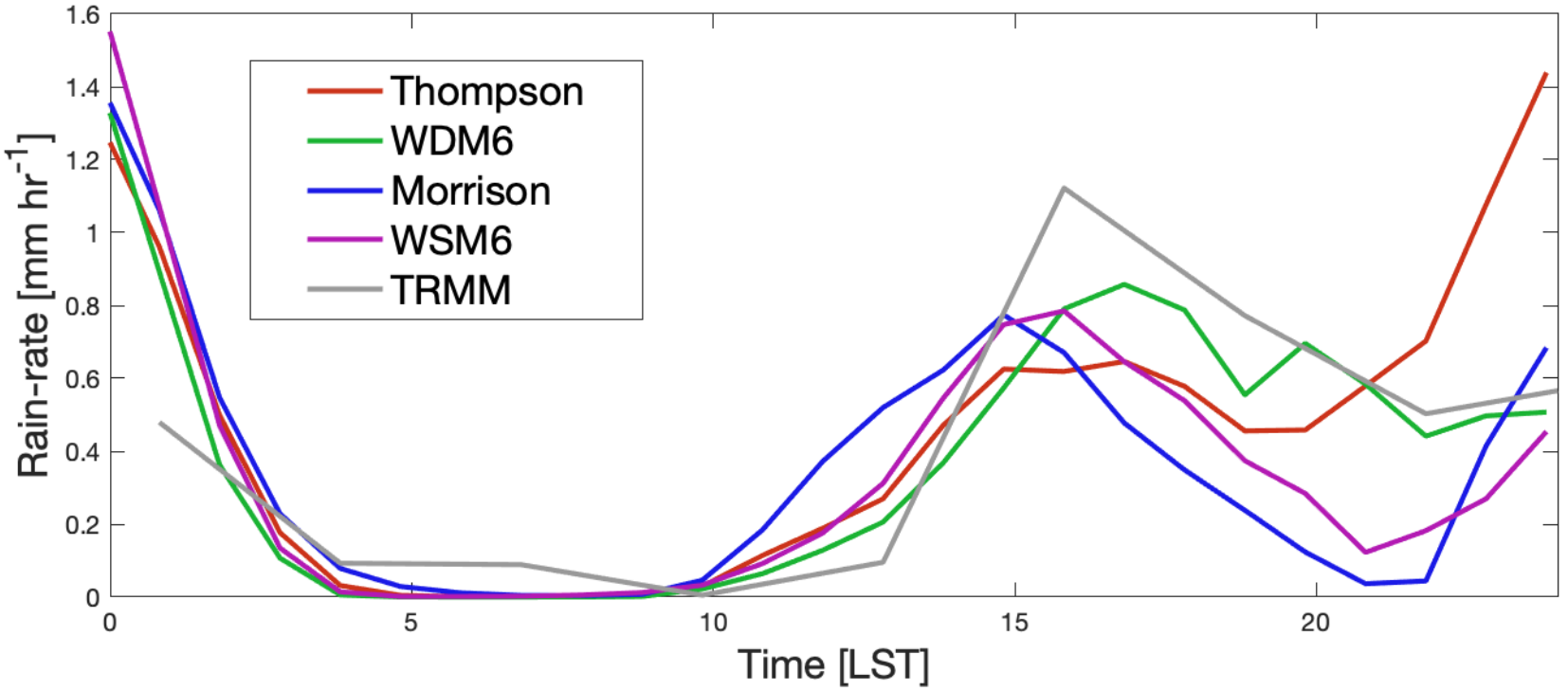

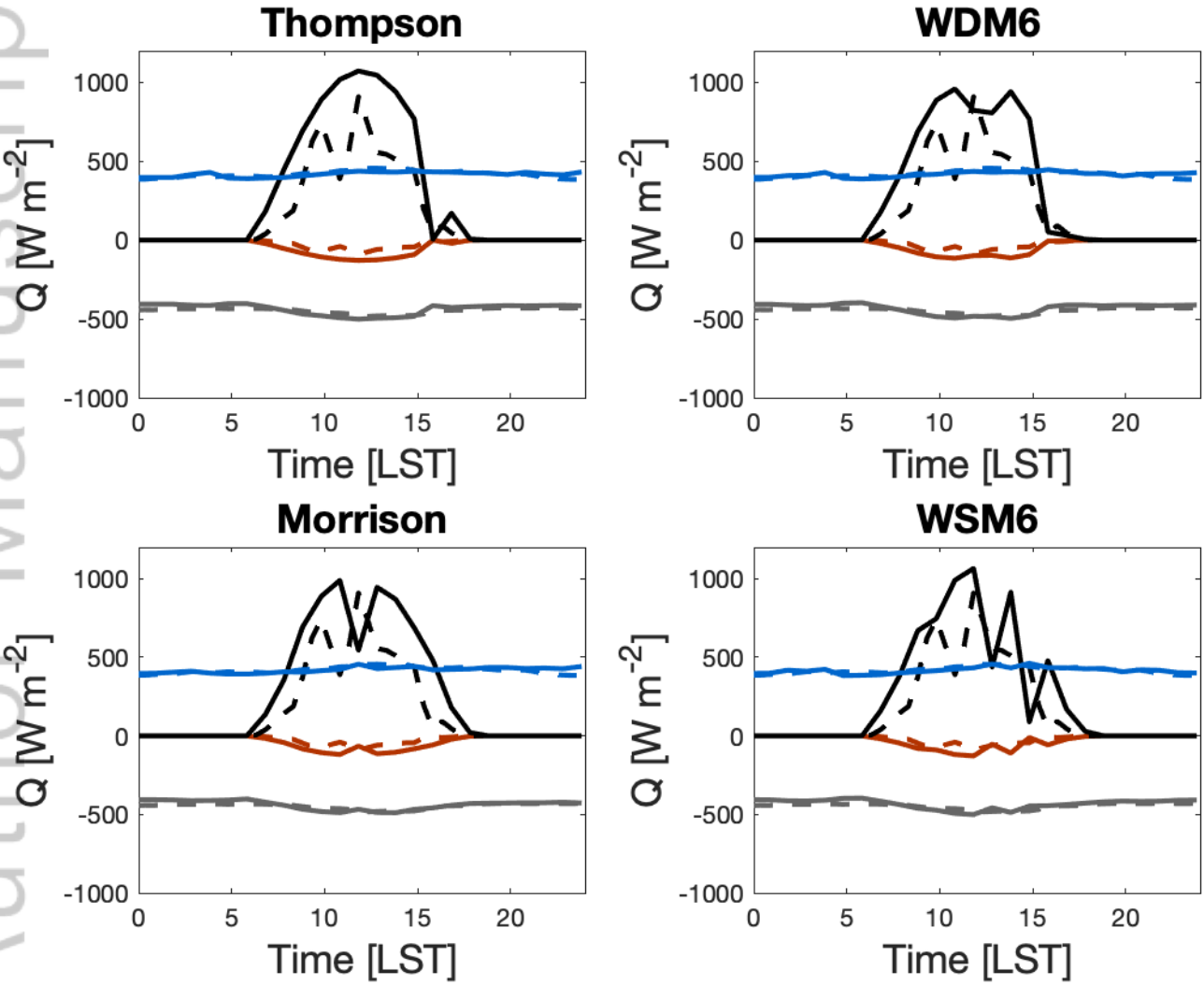

Meso- and micro-scale response to variation in cloudiness at three forested sites in the Maritime Continent

Claire Vincent* and Yi Huang

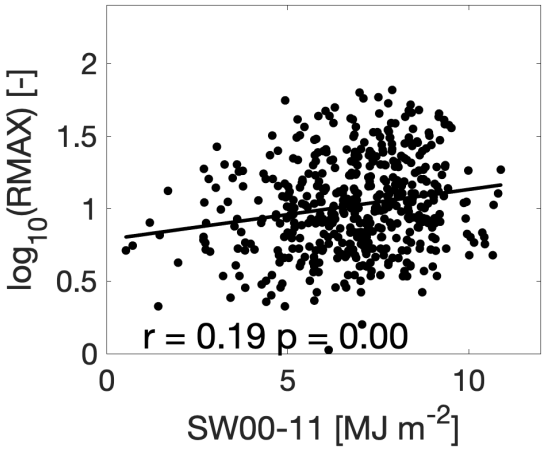

Our study demonstrated that at two inland, forested sites in the Maritime Continent, days with greater incoming shortwave radiation in the morning were positively correlated with a heavier afternoon rainfall peak. This result demonstrates the local controls on precipitation in the tropics. These local controls contribute to the way in which changes in large-scale cloud environments modulate the diurnal precipitation cycle in the Maritime Continent.